Catal Lett (2012) 142:975–983
DOI 10.1007/s10562-012-0850-0

Low Pt Loading High Catalytic Performance of PtFeNi/Carbon Nanotubes Catalysts for CO Preferential Oxidation in Excess Hydrogen I: Promotion Effects of Fe and/or Ni

Limin Chen · Ding Ma · Zhen Zhang · Yuanyuan Guo · Daiqi Ye · Bichun Huang

Received: 30 March 2012 / Accepted: 28 May 2012 / Published online: 12 June 2012

Abstract The commercial carbon nanotubes (CNTs-o) and purified carbon nanotubes (CNTs-p) have been utilized to prepare Pt(FeNi)/CNTs catalysts for CO preferential oxidation (PROX) in H_2 rich stream. The 3 wt%Pt0.41 %Fe 0.35 %Ni/CNTs-p catalyst after activation at 500 °C in H_2 can almost completely remove CO at 6 °C in feed gas containing 1 % CO, 0.5 % O_2 (volume ratio) and H_2 balance. CNTs-o supported 3 wt% Pt can also remove CO almost completely at room temperature, after activation at 500 °C in the feed gas. And this catalyst can keep high activity, high selectivity and high stability for PROX of CO at room temperature. These catalysts are the most effective catalysts for PROX of CO with much lower Pt loading until so far. H-TPR, XRD, HRTEM and reaction results indicate that the Fe and/or Ni precursors have been reduced to metallic state after activation in H_2 which can be oxidized to coordinatively unsaturated FeOx and/or NiOx active species after exposure to feed gas. XPS data point out that over oxidation of Fe and Pt species will deactivate the catalysts seriously. The high catalytic performance is mainly due to the promotion effects of in situ formed coordinatively unsaturated FeOx and/or NiOx species and the unique properties of CNTs.

Keywords Low Pt loading · Fe/Ni promoted Pt catalysts · Carbon nanotubes · CO preferential oxidation (PROX)

1 Introduction

Proton exchange membrane fuel cells (PEMFCs), operating at relatively low temperatures (e.g., 60–80 °C) with pure hydrogen or reformed gas as fuels, have attracted much attention as a potential power source for electric vehicles [1–4]. However, when the PEMFC feed stream is produced by reforming of methanol and hydrocarbons, the gas always contains some amount of CO as an impurity, which is a poison for the fuel cell anode catalysts. Therefore, the CO must be removed before it is supplied to the fuel cell system. Several methods for the CO removal have been studied and recently reviewed by Park et al. [5]: selective H_2-diffusion through membranes, CO methanation and selective oxidation, also known as CO preferential oxidation (PROX) reaction. Among these methods, the PROX process has been considered as the most promising and cost effective one. Especially, in recent years the outstanding catalytic performances of noble metals for PROX of CO, such as Pt, Rh, and Au, have been widely recognized [5–7]. Among them, it has been reported that the catalytic activities of 4 wt% or higher Pt based catalysts could be significantly enhanced by the addition of 2nd metals at low temperatures, such as Fe [8–11], Co [12–14], Ni [15, 16], Ce [17, 18], Mn [15, 19] and alkali metals

Electronic supplementary material The online version of this article (doi:10.1007/s10562-012-0850-0) contains supplementary material, which is available to authorized users.

L. Chen (✉) · Y. Guo · D. Ye · B. Huang
Guangdong Provincial Key Laboratory of Atmospheric Environment and Pollution Control, College of Environmental Science and Engineering, South China University of Technology, Guangzhou 510006, China
e-mail: liminchen@scut.edu.cn

L. Chen · D. Ma · Z. Zhang
State Key Laboratory of Catalysis, Dalian Institute of Chemical Physics, Chinese Academy of Sciences, Dalian 116023, China

D. Ma
College of Chemistry and Molecular Engineering, Peking University, Beijing 100871, China

[20–22] etc. Our previous work has already demonstrated that coordinatively unsaturated ferrous (CUF) sites confined in nanosized matrices can completely remove 1 % CO in H_2 with stoichiometric O_2 at room temperature [11]. It is worth mentioning that most of published work was focused on oxide and zeolite supports and only very limited publications report carbon materials as supports [16].

In fact, carbon materials as the support for metal catalysts are more attractive because of most carbon materials are electron conductive, which enables carbon-supported catalysts be integrated directly into fuel cells [23, 24]. Importantly, carbon nanotubes (CNTs) have more unique properties superior to these inorganic supports, such as unique electrical conductivity, stability and high specific surface area. Furthermore, some papers have reported that CNTs deserve as catalyst [25] and catalyst supports [26–29] in heterogeneous catalysis, particularly hydrogen involved reactions, such as fuel cells [3, 4], NH_3 synthesis and decomposition [26, 27] etc. The high graphitization of CNTs [28] and the electron transfer between active metals and CNT supports [29] have been proposed to be responsible for the superior catalytic activity of the supported catalysts.

In addition, Fe and/or Ni usually used as catalysts during CNTs preparation [30] and these catalyst residues have also been considered to present comparable with or better catalytic activities than commercial catalyst for NH_3 decomposition [26]. Here, we report the high catalytic performances of PtFeNi/CNTs catalysts with much lower Pt loading for CO PROX with stoichiometric O_2 at lower temperature, compared with our previous $PtFe/SiO_2$ catalyst [11].

2 Experimental

2.1 CNTs-p Preparation

Multi-walled CNTs with 4–8 nm i.d. and 10–20 nm o.d. were purchased from Chengdu Organic Chemicals Co., LTD, China, denoted as CNTs-o. ICP analysis showed there were 0.41 wt% Fe and 0.35 wt% Ni residues in original CNTs (CNTs-o) samples. CNTs oxidation treatment or purification was obtained by a procedure adapted from the literature [27]. 3 g CNTs-o (as received) were suspended in 150 ml concentrated nitric acid (68 wt%) and refluxed at 140 °C in an oil bath for 14 h. After the mixture was cooled down to room temperature, it was filtered through a PTFE film with a pore diameter of 0.2 μm and washed with deionized water until the pH value of the filtrate was around 7. Then the product was dried at 60 °C for 12 h. This treatment removes the catalyst residues as well as amorphous carbon. At the same time, surface oxygen functional groups such as carbonyl, carboxylic and ether are introduced onto the surfaces of the CNTs [24]. The sample after purification was further treated in He at 600 °C for 3 h and the obtained sample was labeled as CNTs-p.

2.2 Catalyst Preparation

Pt/CNTs-o catalysts were prepared by conventional wetness impregnation method using ethanol solution of hexachloroplatinic acid (Shenyang Chemical Reagent Company, AR) according to the metal loadings, followed by drying at 120 °C for 12 h. The PtFeNi/CNTs-p catalyst was prepared by the sequential wetness impregnation method, impregnated with ethanol solution of hexachloroplatinic acid followed by drying at 120 °C for 12 h and then impregnated with ethanol solution of ferric nitrate and nickel nitrate mixture. All catalyst preparation was conducted at room temperature. The catalysts were pretreated in H_2 or feed gas [1 % CO, 0.5 % O_2 (volume ratio) and balanced with H_2] at 500 °C for 2 h before catalytic tests.

2.3 Activity Test

The catalytic reactions were evaluated in a fixed-bed flow reactor. A small quartz tube containing a thermocouple was placed in the middle of the catalyst bed. For PROX of CO, gas mixture containing 1 % CO, 0.5 % O_2 (volume ratio) and balanced with H_2 was fed at a flow rate of 25 ml/min, passing through 0.060 g catalyst bed. For CO oxidation reactions, the gas mixture consists of 1.06 % CO, 0.50 % O_2 (volume ratio) and balanced with He or 1.0 % CO, 20 % O_2 (volume ratio) and balanced with He. The composition of the effluent gas was monitored by an on-line gas chromatograph (Agilent Technologies GC-6890N) equipped with PN and TDX-01 columns. Besides the feed, only two products, CO_2 and H_2O, were detected by TCD detector with minimum CO detection limit of 20 ppm. CO and O_2 conversions were calculated from the differences between their inlet and outlet concentrations, respectively, while the selectivity toward CO oxidation (S) is defined as the fraction of oxygen consumed to oxidize CO to CO_2:

$$S = \left\{0.5 \times \left([CO]_{in} - [CO]_{out}\right) / \left([O_2]_{in} - [O_2]_{out}\right)\right\} \times 100\,\%,$$

where $[O_2]_{in}$ and $[CO]_{in}$ are inlet and $[O_2]_{out}$ and $[CO]_{out}$ are outlet concentrations of O_2 and CO, respectively.

2.4 Catalyst Characterization

XRD measurements were carried out on a Rigaku D/Max 2500 diffractometer with a Cu K_α monochromatized radiation source, operated at 40 kV and 250 mA. The

transmission electron microscopy (TEM, TECNAI Spitrit) and the high resolution transmission electron microscopy (HRTEM, TECNAI F30) were utilized to characterize the morphological, structural properties and catalyst particle sizes of the samples. Temperature programmed reduction (TPR) measurements were conducted in a fixed bed quartz reactor containing 60 mg of sample at a heating rate of 10 °C/min, from 60 to 800 °C, in 10 % hydrogen diluted in argon (30 ml/min) as a reducing gas. The TPR profile was monitored continuously with an on-line TCD-GC. XPS analysis was performed on an Amicus spectrometer with the Mg K_α radiation (1253.6 eV), operating at 12.5 kV and 250 W. The surface charging effect was corrected by fixing the C 1s peak at a binding energy of 284.6 eV.

3 Results and Discussion

3.1 The High Catalytic Performance of Pt/CNTs-o Catalysts

Figure 1 shows O_2 conversion (A), CO conversion (B) and selectivity (C) as a function of the reaction temperature over Pt/CNTs-o catalysts with different Pt loadings. The CNTs-o was also evaluated for the PROX of CO reaction; however, no visible catalytic activity was observed. All Pt catalysts presented good catalytic activity compared with purified CNTs, inorganic oxides or zeolites supported Pt catalysts. For 1 wt% Pt/CNTs-o catalyst, oxygen reached full conversion at about 100 °C and CO reached the maximum conversion about 80 % at the same temperature. For 2 wt% Pt/CNTs-o catalyst, oxygen was completely converted at around 90 °C and more than 85 % CO was removed. This means even very low Pt loading catalyst can remove large amounts of CO under PEMFCs operation temperature. When the Pt loading was increased to 3 wt%, nearly 100 % O_2 and CO conversion were obtained at room temperature (23 °C).

Figure 2 shows O_2 conversion (A), CO conversion (B) and Selectivity (C) versus time on stream over the Pt/CNTs-o samples with different Pt loadings. 1 and 2 wt% Pt/CNTs-o were tested at 100 °C after the reaction from 23 to 180 °C. The catalysts gave 100 and 80–85 % initial O_2 and CO conversions, respectively; O_2 and CO conversions decreased gradually along the time. 3 and 4 wt% Pt/CNTs-o were evaluated at 23 °C. The initial O_2 and CO conversions were both nearly 100 % over these two catalysts. 3 wt% Pt/CNTs-o sample exhibited relatively better stability among these four samples. O_2 conversion began to decrease after reaction for 280 min; CO conversion was still above 90 % even after reaction for 5 h.

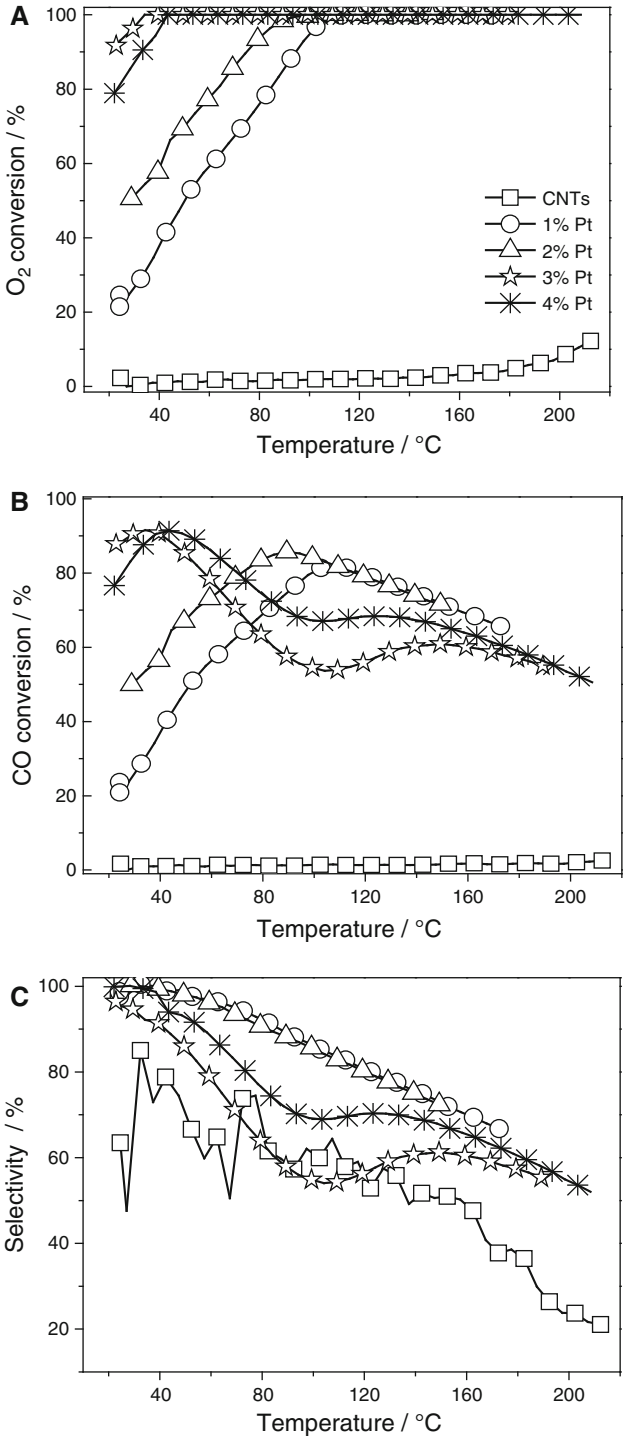

Fig. 1 Variation of O_2 conversion (**a**), CO conversion (**b**), and selectivity S (**c**) as a function of the reaction temperature over Pt/CNTs-o catalysts with different Pt loadings. Before the catalytic evaluation, the samples were pretreated in H_2 at 500 °C for 2 h. 3 wt% Pt and 4 wt% Pt catalysts were tested after reaction at room temperature (23 °C) for 5 h

It is interesting to find that above catalysts present better catalytic performance after reaction at high temperatures. And our previous research also demonstrates

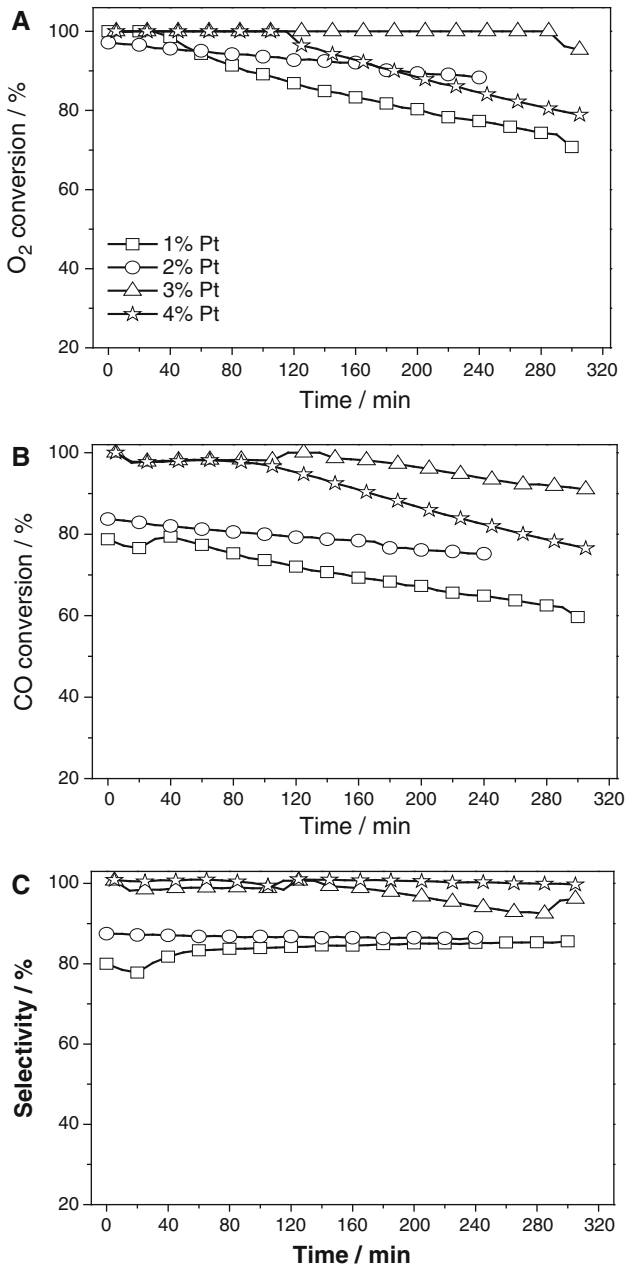

Fig. 2 O_2 conversion (**a**), CO conversion (**b**) and Selectivity S (**c**) versus time on stream over Pt/CNTs-o catalysts with different Pt loadings after activation in H_2 at 500 °C for 2 h. 1 wt% Pt and 2 wt% Pt were tested at 100 °C after the reaction from room temperature to 180 °C; 3 wt% Pt and 4 wt% Pt were tested at room temperature

that catalysts will exhibit better catalytic performance after activation in CO PROX feed gas [31]. So, we have evaluated PROX of CO reaction after catalyst activation in feed gas. Figure 3 gives the CO conversion and selectivity versus time on stream for PROX of CO at room temperature over 3 wt% Pt/CNTs-o sample after activation in feed gas at 500 °C for 2 h. As presented, both CO conversion and selectivity keep nearly 100 % during the test period, and CO can be almost completely

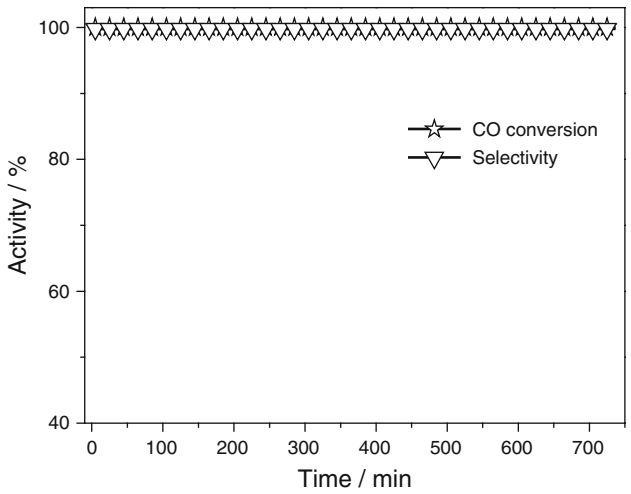

Fig. 3 The time-on-stream behaviors of 3 wt% Pt/CNTs-o catalyst after activation in feed gas at 500 °C for 2 h for PROX of CO at room temperature (23 °C)

removed at room temperature in the existence of stoichiometric ratio O_2. This means that 3 wt% Pt/CNTs-o has high activity, high selectivity and high stability with stoichiometric ratio O_2 at room temperature for PROX of CO. This catalyst presents better or comparable catalytic performance than that of others in the previous publications with much lower Pt loading. As mentioned above, both the unique properties of CNTs (confinement effects and electron effects etc.) and Fe/Ni catalyst residues may facilitate Pt catalyst for PROX of CO. Here, in order to clarify the effects of Fe/Ni on the catalytic performances, the purified CNTs, CNTs-p, was used to prepare 3 wt% Pt/CNTs-p (Pt/CNTs-p) and 3 wt% Pt 0.41 wt% Fe 0.35 wt% Ni/CNTs-p (PtFeNi/CNTs-p) catalysts.

3.2 The Promotion Effects of Fe and/or Ni on Catalytic Performance

Figure 4 gives catalytic properties of Pt/CNTs-p, and PtFeNi/CNTs-p catalysts at different reaction temperatures after activation in H_2 at 500 °C for 2 h. The Pt/CNTs-p catalyst had about 40 % O_2 and CO conversion at 23 °C; the same sample gave about 96 and 78 % O_2 and CO conversion at 124 °C, respectively. As expected, 100 % O_2 conversion and 85 % CO conversion were obtained at 23 °C over PtFeNi/CNTs-p catalyst; further research indicated that almost full O_2 and CO conversions were achieved at 6 °C, much higher catalytic performance than that of Pt/CNTs-p catalyst under the same reaction conditions. These results mean that Fe and/or Ni have significantly enhanced the catalytic performance of Pt catalyst. This is the most effective catalyst for PROX of CO with much lower Pt loading until so far.

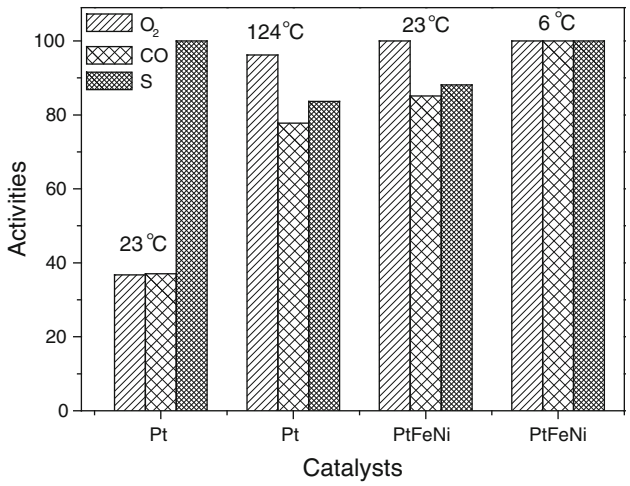

Fig. 4 The O_2 conversion (O_2), CO conversion (CO) and Selectivity (S) over 3 wt% Pt/CNTs-p (Pt) and 3 wt% Pt 0.41 wt% Fe 0.35 wt% Ni/CNTs-p (PtFeNi) catalysts at different reaction temperatures after activation in H_2 at 500 °C for 2 h

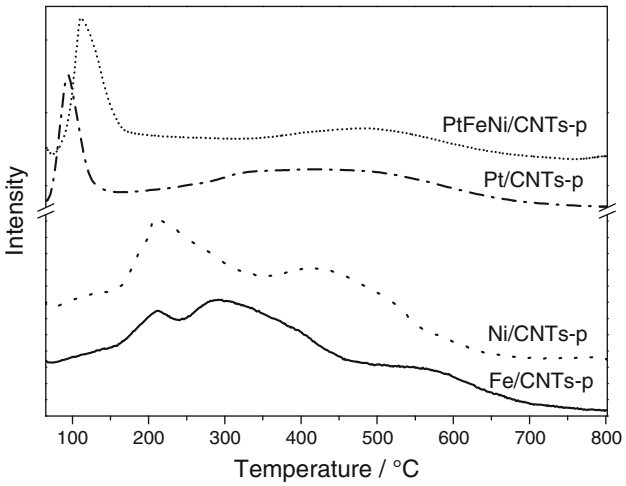

Fig. 5 H-TPR profiles of fresh Fe/CNTs-p, Ni/CNTs-p, Pt/CNTs-p and PtFeNi/CNTs-p catalysts

4 Discussion

4.1 The Promotion Effects of FeOx and/or NiOx

4.1.1 The Chemical States of Pt, Fe and Ni After Activation

Our previous research demonstrated the highly active and stable PtFe/SiO_2 catalyst after activation in H_2 at 200 °C. And the CUF sites confined in nanosized matrices structure contribute to the high activity, high selectivity and high stability [11]. The literature reported [8–11] that Mordenite, SiO_2 etc. supported Pt and Fe and/or Ni catalyst exhibited high activity for PROX of CO after activation in H_2 or air at low temperature (200–300 °C). FeOx has been confirmed to promote PROX reaction and bifunctional mechanism has been proposed for these catalytic systems, i.e. Pt and FeOx adsorb CO and O_2, respectively [8–11].

However, all of the catalysts were activated in H_2 or CO PROX feed gas at much higher temperature (500 °C), in this article. Then, what's the active state of Fe and Ni here? Figure 5 presents H-TPR curves of fresh Fe/CNTs-p, Ni/CNTs-p, Pt/CNTs-p and PtFeNi/CNTs-p catalysts. Fe/CNTs-p exhibits three hydrogen consumption peaks clearly. The first peak, centered at around 210 °C, can be assigned to the reduction of Fe_2O_3 to Fe_3O_4. The second peak, centered at around 290 °C, can be ascribed to the subsequent reduction of Fe_3O_4 to FeO. The third peak, observed at 500–600 °C, can be related to the reduction of FeO to metallic Fe and gasification of CNTs at a temperature higher than 600 °C [32]. Ni/CNTs-p catalyst displays two hydrogen consumption peaks. According to the literature [33], the lower temperature reduction peak at around 210 °C is corresponded to the reduction of nickel which originally was present as nitrate. The reduction above about 350 °C, is due to some nickel catalyzed carbon gasification. For Pt/CNTs-p, a first hydrogen consumption peak at low temperature ($\sim$100 °C) is attributed to the reduction of platinum species to the metallic state. A second broader consumption peak is observed at higher temperatures, in the range of 300–550 °C. It is generally accepted that during and after the reduction of Pt hydrogen is chemisorbed on the metal and then spilt over the surface of the support, occupying unsaturated reactive sites originated by the decomposition of surface oxygen groups, and additionally by some carbon gasification [34]. The H-TPR profile of PtFeNi/CNTs-p catalyst is similar to the reported activated carbon supported PtFe bimetal catalyst, Pt, Fe and Ni species were reduced simultaneously at much lower temperature than that of Fe and Ni species [35]. H-TPR results indicate that Pt, Fe and Ni are all metallic form after activation in H_2 at 500 °C.

Figure 6 show XRD patterns of CNTs-o and 3 wt% Pt/CNTs-o after activation in H_2 at 500 °C. A shoulder located at 39.8° can be observed clearly, which is attributed to the diffraction of metallic Pt. There is no shift of 2θ compared with metallic Pt which means no significant alloy has been formed. No Fe and Ni diffraction peaks were detected either. Figure 7 presents TEM and HRTEM images of 3 wt% Pt/CNTs-o after activation in H_2 at 500 °C. It is obvious that nanoparticles are located both inside and outside the channels of CNTs and the average diameter is smaller than 2 nm (Fig. 7a–c). The HRTEM image (Fig. 7d) shows that 3 wt% Pt/CNTs-o sample presents face-centered cubic (FCC) Pt lattice with a Pt(111) interlayer spacing of 2.23 A. This means that the nanoparticles are still dominated by metallic Pt. Combined with

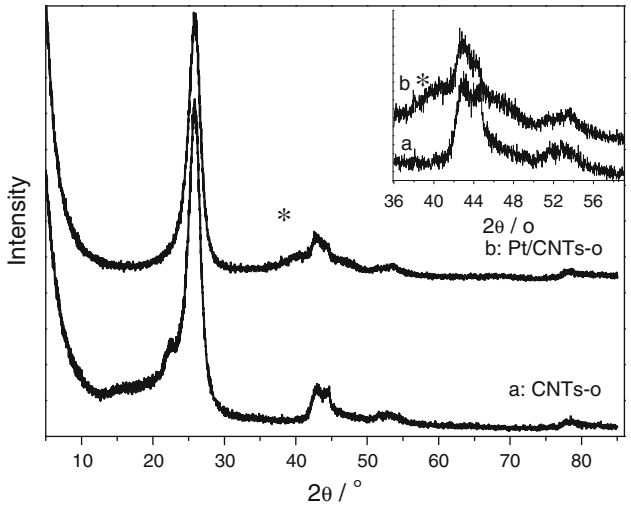

Fig. 6 XRD patterns of CNTs-o and 3 wt% Pt/CNTs-o catalysts after activation in H_2 at 500 °C for 2 h. The *inset* is their XRD patterns in the range from 36 to 59°

H-TPR results, it is clear that Pt, Fe and Ni are all metallic form after activation in H_2 at 500 °C. This is quite different from our previous published $PtFe/SiO_2$ system.

4.1.2 *The Chemical States of Pt, Fe and Ni After Exposure to Feed Gas*

The oxidation process of CNTs supported Fe has been investigated in 1 vol% O_2 balanced with He by in situ XRD [36]. The results demonstrates that CNTs supported Fe can be oxidized to Fe_2O_3 at around 100 °C and obvious oxidation reaction occurs even under 90 °C. Chen et al. [37] calculated the stability of the Pt-3d-Pt(111) (3d = Ti, V, Cr, Mn, Fe, Co, or Ni) bimetallic surface structures in the presence of adsorbed oxygen by means of density functional theory (DFT). Their calculation predicts that all of the Pt-3d-Pt(111) subsurface structures are thermodynamically unstable with adsorbed oxygen. The segregation for 3d metal atoms from Pt-3d-Pt(111) to 3d-Pt-Pt(111) will occur when exposed to a half monolayer of oxygen. The activation barrier of the segregation of subsurface Ni atoms was determined to be only 15 ± 2 kcal/mol. They also confirmed their predictions experimentally by using Auger electron spectroscopy (AES) and high-resolution electron energy loss spectroscopy (HREELS). Bao et al. also observed Fe segregation from subsurface on Pt(111) to form FeOx after exposure to proper amount of O_2 [38]. All of these investigations indicate that Fe/Ni can be oxidized to FeOx and/or NiOx species after being exposed to low O_2 partial pressure or feed gas at low temperature.

In order to confirm the high active sites are related to in situ formed coordinatively unsaturated FeOx and/or NiOx species, the time on stream behaviors of CO oxidation in different O_2 partial pressure at 23 °C was carried out over 3 wt% Pt/CNTs-o after activation in H_2 at 500 °C for 2 h. As shown in Fig. 8, the initial CO conversion was 94 % while O_2 was consumed completely in the reaction mixture containing 1.06 % CO, 0.5 % O_2 (volume ratio), 98.44 % He. CO was not fully converted mainly because of the shortage of O_2 in the feeding gas. CO conversion decreased gradually along with the reaction time and it was about 70 % after reaction for 5 h. On the contrary, in the reaction mixture 1 % CO, 20 % O_2 (volume ratio), He balance, 100 % initial CO conversion was obtained but it dropped to 50 % quickly then decreased gradually along the time. After 5 h, CO conversion was only about 30 %. Combined with time on stream behaviors of CO PROX reaction, it seems that the catalyst loses activity much faster in higher O_2 partial pressure. The reductive reaction atmosphere and/or lower O_2 partial pressure favors CO oxidation which may be due to that the highly active site is related to the metastable state of Fe and Ni and H_2 may be benefit to maintain the metastable state species. In addition, the high activity, high selectivity and high stability of 3 wt% Pt/CNTs-o catalyst after activation in feed gas at 500 °C at room temperature also testifies the formation of coordinatively unsaturated FeOx and/or NiOx species during activation and the high activation temperature may be helpful to the generation of stable structure, then leading to stable high catalytic performance. Therefore, the PtFeNi/CNTs catalyst is an efficient catalyst for PROX of CO and the high catalytic performance may also originate from the formation of coordinatively unsaturated FeOx and/or NiOx species.

In order to further clarify the highly active site is related to the metastable state of Fe and Ni, XPS has been used to determine the chemical states of 3 wt% Pt/CNTs-o catalyst after activation in H_2 at 500 °C for 2 h then exposed to air at room temperature, as shown in Fig. 9. The XPS survey scan only detected the existence of C, O, Pt and Fe. The binding energy of Pt $4f_{7/2}$ and Fe $2p_{3/2}$ are 72.7 and 711.2 eV, respectively, which can be attributed to Pt(II)Ox and Fe(III) OOH, respectively [11, 15]. These results indicated that both Pt and Fe on the surface of the catalyst were oxidized after exposure to air at room temperature. This means the over oxidation of Fe and Pt may deactivate the catalytic performance and coordinatively unsaturated FeOx and/or NiOx species may be only produced by exposing metallic state Fe/Ni to low oxygen partial pressure.

4.2 The Much Lower Pt Loading

Both promotion effects of Fe and/or Ni and the unique properties of CNTs contribute to the high catalytic performance of PtFeNi/CNTs-p on PROX of CO from our

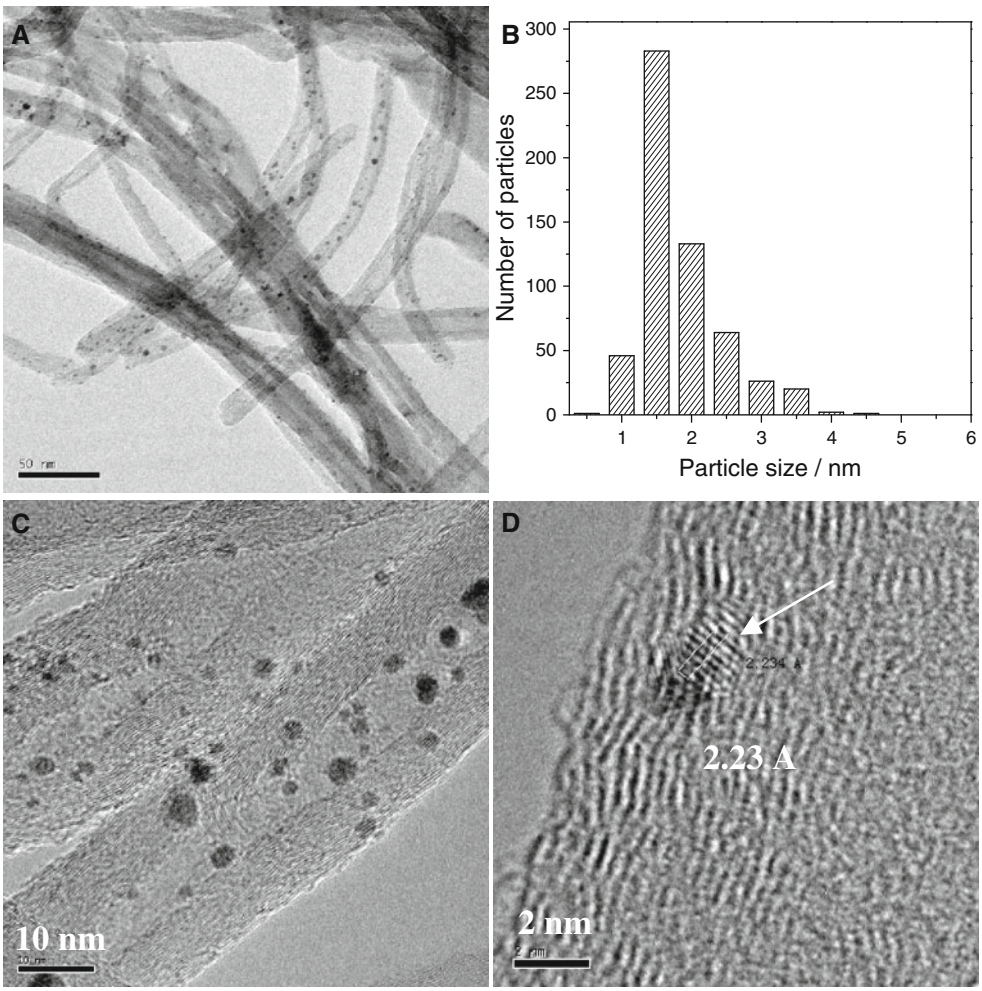

Fig. 7 TEM (**a**), particle size distribution (**b**) and HRTEM (**c**, **d**) images of 3 wt% Pt/CNTs-o catalyst after activation in H_2 at 500 °C for 2 h

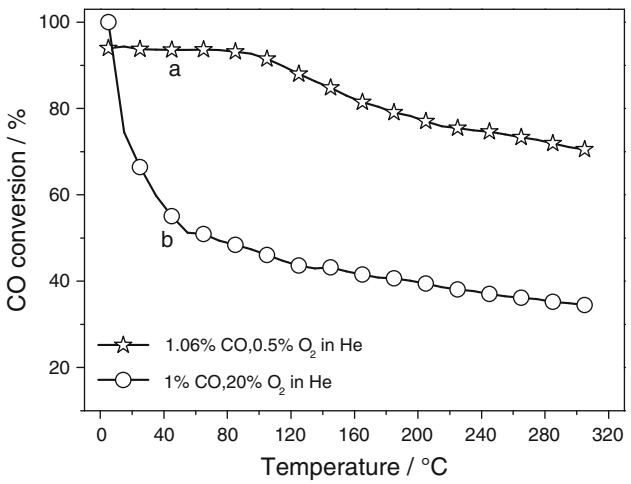

Fig. 8 The time-on-stream behaviors of 3 wt% Pt/CNTs-o at 23 °C after activation in H_2 at 500 °C for 2 h for CO oxidation with different O_2 partial pressures

research. The H-TPR, XRD, HRTEM, XPS and the designed reaction results demonstrate that promotion effects of FeOx and/or NiOx mainly originate from the formation of coordinatively unsaturated FeOx and/or NiOx species. In this article, PtFeNi/CNTs-p catalyst can almost completely remove CO in 1.0 % CO, 0.5 % O_2 (volume ratio), 98.5 % H_2 with 3 wt% Pt at 6 °C, with much higher catalytic performance and significantly lower loading than other reported catalytic systems[8–11]. In the previous publications [8–11], 4 or 5 wt% Pt were usually loaded over SiO_2 or Al_2O_3 etc. It is well known that there is great difference between SiO_2 or Al_2O_3 and CNTs supports, so it is hard to make comparisons. Then, carbon materials were used and among them, CNTs-p supported catalyst gave the best catalytic performance. These results mean that the unique properties of CNTs also contribute a lot to the much lower Pt loading. The effects of CNTs on high catalytic performance for PROX of CO will be published elsewhere in details.

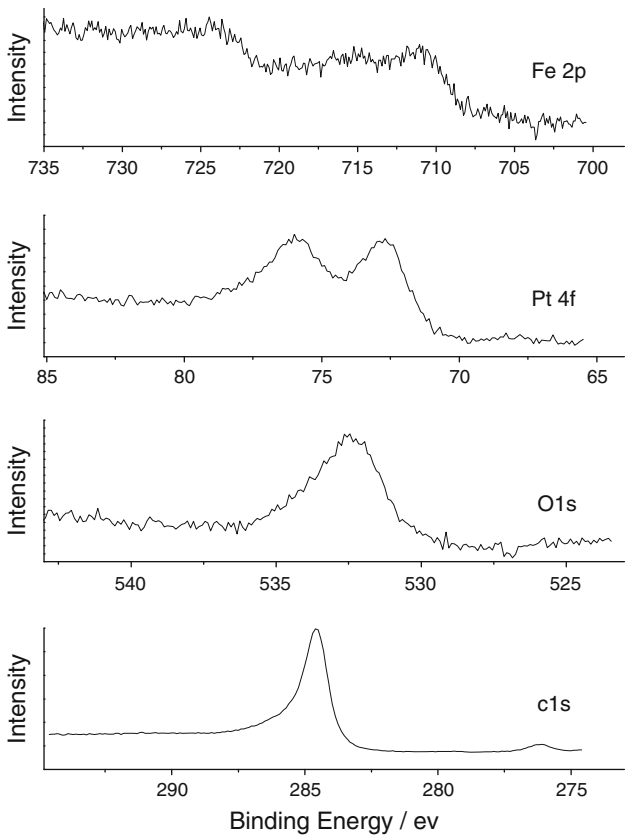

Fig. 9 XPS spectra of Fe 2p, Pt 4f, O 1s and C 1s of 3 wt% Pt/CNTs-o catalyst after activation in H_2 at 500 °C for 2 h then exposed to air at room temperature

5 Conclusions

In summary, CNTs-p supported Fe and Ni promoted 3 wt% Pt catalysts can almost completely remove CO from rich H_2 stream with stoichiometric ratio O_2 at 6 °C. 3 wt% Pt/CNTs-o catalyst can keep high activity, high selectivity and high stability for PROX of CO at room temperature after activation at 500 °C in the feed gas. The investigation shows that the promotion effects of Fe and/or Ni contribute a lot to the high catalytic performance of PtFeNi/CNTs on PROX of CO, even with much lower Pt loading. The Fe and/or Ni precursors have been reduced to metallic state after activation, which may in situ form coordinatively unsaturated FeOx and/or NiOx species after exposure to feed gas or low O_2 partial pressure gas, then enhance the catalytic performance drastically. The contribution of unique properties of CNTs on the much lower Pt loading and high catalytic performances for PROX of CO will be discussed in details in another paper.

Acknowledgments The authors gratefully thank Dr. Xinhe Bao and Dr. Xiulian Pan at Dalian Institute of Chemical Physics, Chinese Academy of Sciences, for their enthusiastic supervision and helpful discussions. This work is financially supported by the Natural Science Foundation of Guangdong Province, China (Grant No. S2011010000737), the Doctoral Fund of Ministry of Education of China (20110172120017), the Fundamental Research Funds for the Central Universities (Grant No. 2011zm 0048), and the Key Laboratory of Renewable Energy and Gas Hydrate, Chinese Academy of Sciences (No. Y007K1).

References

1. Bing YH, Liu HS, Zhang L, Ghosh D, Zhang JJ (2010) Nanostructured Pt-alloy electrocatalysts for PEM fuel cell oxygen reduction reaction. Chem Soc Rev 39:2184–2202
2. Devanathan R (2008) Recent developments in proton exchange membranes for fuel cells. Energy Environ Sci 1:101–119
3. Antolini E (2009) Carbon supports for low-temperature fuel cell catalysts. Appl Catal B 88:1–24
4. Shao YY, Sui JH, Yin GP, Gao YZ (2008) Nitrogen-doped carbon nanostructures and their composites as catalytic materials for proton exchange membrane fuel cell. Appl Catal B 79:89–99
5. Park ED, Lee D, Lee HC (2009) Recent progress in selective CO removal in a H_2-rich stream. Catal Today 139:280–290
6. Bion N, Epron F, Moreno M, Marino F, Duprez D (2008) Preferential oxidation of carbon monoxide in the presence of hydrogen (PROX) over noble metals and transition metal oxides: advantages and drawbacks. Top Catal 51:76–88
7. Bulushev DA, Yuranov I, Suvorova EI, Buffat PA, Kiwi-Minsker L (2004) Highly dispersed gold on activated carbon fibers for low-temperature CO oxidation. J Catal 224:8–17
8. Siani A, Alexeev OS, Lafaye G, Amiridis MD (2011) The effect of Fe on SiO_2-supported Pt catalysts: structure, chemisorptive, and catalytic properties. J Catal 266:26–38
9. Kotobuki M, Watanabe A, Uchida H, Yamashita H, Watanabe M (2005) Reaction mechanism of preferential oxidation of carbon monoxide on Pt, Fe, and Pt–Fe/mordenite catalysts. J Catal 236:262–269
10. Siani A, Captain B, Alexeev OS, Stafyla E, Hungria AB, Midgley PA et al (2006) Improved CO oxidation activity in the presence and absence of hydrogen over cluster-derived PtFe/SiO_2 catalysts. Langmuir 22:5160–5167
11. Fu Q, Li WX, Yao YX, Liu HY, Su HY, Ma D et al (2010) Interface-confined ferrous centers for catalytic oxidation. Science 328:1141–1144
12. Wang C, Li B, Lin HQ, Yuan YZ (2012) Carbon nanotube-supported Pt-Co bimetallic catalysts for preferential oxidation of CO in a H_2-rich stream with CO_2 and H_2O vapor. J Power Sources 202:200–208
13. Ko EK, Park ED, Lee HC, Lee D, Kim S (2007) Supported Pt-Co catalysts for selective CO oxidation in a hydrogen-rich stream. Angew Chem Int Ed 46:734–737
14. Ding ZX, Yang HY, Liu JF, Dai WX, Chen X, Wang XX, Fu XZ (2011) Promoted CO oxidation activity in the presence and absence of hydrogen over the TiO_2-supported Pt/Co-B bicomponent catalyst. Appl Catal B 101:326–332
15. Mu RT, Fu Q, Xu H, Zhang H, Huang YY, Jiang Z, Zhang S, Tan DL, Bao XH (2011) Synergetic effect of surface and subsurface Ni species at Pt-Ni bimetallic catalysts for CO oxidation. J Am Chem Soc 133:1978–1986
16. Ko EY, Park ED, Seo KW, Lee HC, Lee D, Kim S (2006) Pt–Ni/γ-Al_2O_3 catalyst for the preferential CO oxidation in the hydrogen stream. Catal Lett 110:275–279
17. Şimşek E, Özkara S, Aksoylu AE, Önsan ZI (2007) Preferential CO oxidation over activated carbon supported catalysts in H_2-rich gas streams containing CO_2 and H_2O. Appl Catal A 316:169–174

18. Gorke O, Pfeifer P (2011) Preferential CO oxidation over a platinum ceria alumina catalyst in a microchannel reactor. Int J Hydrogen Energy 36:4673–4681
19. Ayastuy JL, González-Marcos MP, González-Velasco JR, Gutiérrez-Ortiz MA (2007) MnOx/Pt/Al_2O_3 catalysts for CO oxidation in H_2-rich streams. Appl Catal B 70:532–541
20. Tanaka H, Kuriyama M, Ishida Y, Ito SI, Tomishige K, Kunimori K (2008) Preferential CO oxidation in hydrogen-rich stream over Pt catalysts modified with alkali metals: part I. Catalytic performance. Appl Catal A 343:117–124
21. Pedrero C, Waku T, Iglesia E (2005) Oxidation of CO in H_2–CO mixtures catalyzed by platinum: alkali effects on rates and selectivity. J Catal 233:242–255
22. Kuriyama M, Tanaka H, Ito SI, Kubota T, Miyao T, Naito S et al (2007) Promoting mechanism of potassium in preferential CO oxidation on Pt/Al_2O_3. J Catal 252:39–48
23. Chen LM, Ma D, Bao XH (2007) Hydrogen treatment-induced surface reconstruction: formation of superoxide species on activated carbon over Ag/activated carbon catalysts for selective oxidation of CO in H_2-rich gases. J Phys Chem C 111:2229–2234
24. Chen LM, Ma D, Li XY, Bao XH (2006) Silver catalysts supported over activated carbons for the selective oxidation of CO in excess hydrogen: effects of different treatments on the supports. Catal Lett 111:133–139
25. Zhang J, Liu X, Blume R, Zhang AH, Schlögl R, Su DS (2008) Surface-modified carbon nanotubes catalyze oxidative dehydrogenation of *n*-butane. Science 322:73–77
26. Zhang J, Comotti M, Schüth F, Schlögl R, Su DS (2007) Commercial Fe- or Co-containing carbon nanotubes as catalysts for NH_3 decomposition. Chem Commun 19:1916–1918
27. Guo SJ, Pan XL, Gao HL, Yang ZQ, Zhao JJ, Bao XH (2010) Probing the electronic effect of carbon nanotubes in catalysis: NH_3 synthesis with Ru nanoparticles. Chem Eur J 16:5379–5384
28. Rodriguez NM, Kim MS, Baker RTK (1994) Carbon nanofibers: a unique catalyst support medium. J Phys Chem 98:13108–13111
29. Hung V, Gonçalves F, Philippe R, Lamouroux E, Kihn MCY, Plee D et al (2006) Bimetallic catalysis on carbon nanotubes for the selective hydrogenation of cinnamaldehyde. J Catal 240:18–22
30. Hofmann S, Blume R, Wirth CT, Cantoro M, Sharma R, Ducati C et al (2009) State of transition metal catalysts during carbon nanotube growth. J Phys Chem C 113:1648–1656
31. Qu ZP, Cheng MJ, Shi C, Bao XH (2002) Effects of silver loading and pretreatment with reaction gas on CO selective oxidation in H_2 over silver catalyst. Chin J Catal 23:460–464
32. Abbaslou RMM, Tavasoli A, Dalai AK (2009) Effect of pretreatment on physico- chemical properties and stability of carbon nanotubes supported iron Fischer–Tropsch catalysts. Appl Catal A 355:33–41
33. Silva LMS, Órfão JJM, Figueiredo JL (2001) Formation of two metal phases in the preparation of activated carbon-supported nickel catalysts. Appl Catal A 209:145–154
34. Fraga MA, Jordão E, Mendes MJ, Freitas MMA, Faria JL, Figueiredo JL (2002) Properties of carbon-supported platinum catalysts: role of carbon surface sites. J Catal 209:355–364
35. Mahata N, Gonçalves F, Pereira MFR, Figueiredo JL (2008) Selective hydrogenation of cinnamaldehyde to cinnamyl alcohol over mesoporous carbon supported Fe and Zn promoted Pt catalyst. Appl Catal A 339:159–168
36. Chen W, Pan XL, Bao XH (2007) Tuning of redox properties of iron and iron oxides via encapsulation within carbon nanotubes. J Am Chem Soc 129:7421–7426
37. Menning CA, Hwu HH, Chen JG (2006) Experimental and theoretical investigation of the stability of Pt-3d-Pt(111) bimetallic surfaces under oxygen environment. J Phys Chem B 110:15471–15477
38. Ma T, Fu Q, Cui Y, Zhang Z, Wang Z, Tan DL, Bao XH et al (2010) Controlled transformation of the structures of surface Fe (FeO) and subsurface Fe on Pt(111). Chin J Catal 31:24–32